applied sciences

MDPI

Review

Chalcogenide Microstructured Optical Fibers for Mid-Infrared Supercontinuum Generation: Interest, Fabrication, and Applications

Yiming Wu, Marcello Meneghetti, Johann Troles * and Jean-Luc Adam

CNRS, ISCR-UMR 6226, Univ Rennes, F-35000 Rennes, France; yiming.wu@univ-rennes1.fr (Y.W.); marcello.meneghetti@univ-rennes1.fr (M.M.); Jean-Luc.Adam@univ-rennes1.fr (J.-L.A.)

* Correspondence: johann.troles@univ-rennes1.fr; Tel.: +33-(0)2-2323-6733

Received: 25 July 2018; Accepted: 11 September 2018; Published: 13 September 2018

Abstract: The mid-infrared spectral region is of great technical and scientific importance in a variety of research fields and applications. Among these studies, mid-infrared supercontinuum generation has attracted strong interest in the last decade, because of unique properties such as broad wavelength coverage and high coherence, among others. In this paper, the intrinsic optical properties of different types of glasses and fibers are presented. It turns out that microstructured chalcogenide fibers are ideal choices for the generation of mid-infrared supercontinua. The fabrication procedures of chalcogenide microstructured fibers are introduced, including purification methods of the glass, rod synthesis processes, and preform realization techniques. In addition, supercontinua generated in chalcogenide microstructured fibers employing diverse pump sources and configurations are enumerated. Finally, the potential of supercontinua for applications in mid-infrared imaging and spectroscopy is shown.

Keywords: chalcogenide glasses; chalcogenide fibers; mid-infrared; supercontinuum generation

1. Introduction

The search for supercontinuum (SC) sources reaching into the mid-infrared (mid-IR) region (which covers the 2–20 μm electromagnetic spectral range) has drawn much attention in recent years. This is mainly because the atmospheric transparent windows (3–5 μm and 8–12 μm) and the molecular fingerprint region are included in this range. Thanks to these features, Mid-IR SC is considered to be a new source highly applicable in the fields of spectroscopy, sensing, biology, metrology, and defense [1,2]. Limited in terms of infrared absorption, silica-based SC generation could merely extend their spectral domain above ~2.7 μm [1,3–5]. Meanwhile, several other alternative materials were selected for the realization of Mid-IR SC generation, some of which are soft glasses such as tellurite [6,7], fluoride glasses [8,9], and chalcogenide glasses (ChG) [10–12]. As an example, Martinez et al. reported an all-fiber configuration SC generation with a continuous spectrum from 1.6 to >11 μm and 417 mW on-time average output power, by pumping a cascade of Zr–Ba–La–Al–Na fluoride (ZBLAN) fiber, arsenic sulfide (As_2S_3) fiber, and arsenic selenide (As_2Se_3) fiber with a master oscillator power amplifier (MOPA) [13]. Considering the optical and chemical properties of these materials, chalcogenide glass with its wide transparency in the Mid-IR range and several orders of magnitude higher nonlinearity than standard fused silica [14] surpasses the other glasses. Furthermore, by combining the characteristics of single-mode propagating and more flexible chromatic dispersion modification of microstructured optical fibers (MOF), chalcogenide MOFs would be optimal for Mid-IR SC generation. In this paper, optical transmissions of different fibers are compared, and the advantages of chalcogenide photonic crystal fiber (PCF) for generating Mid-IR supercontinua are introduced and

discussed. Fabrication methods of chalcogenide fibers and chalcogenide PCF are described, and finally, examples of Mid-IR supercontinua generated from these fibers and applications are presented.

2. Why Choose Chalcogenide Microstructured Optical Fibers for Mid-Infrared Supercontinuum Generation?

For the generation of supercontinua in the Mid-IR region, the gain medium or the conversion medium is of great importance, besides the pump source. Generally, there are two sorts of Mid-IR fibers, which are passive fibers and active fibers, respectively. Passive fibers are applied to transmit infrared information, whereas active fibers generate Mid-IR light by using nonlinear effects or rare-earth doping [15]. Figure 1 lists and compares the transmission coverage of several different fibers.

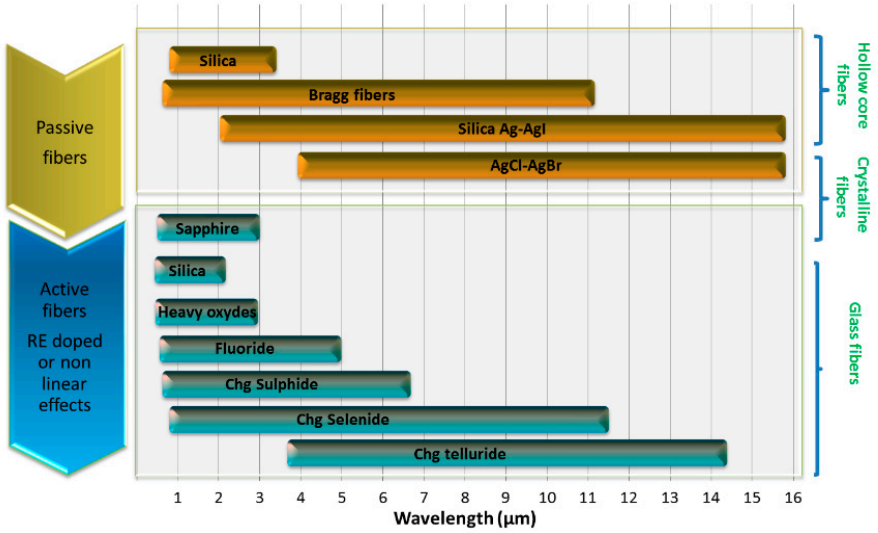

Figure 1. Mid-infrared transmissions of different types of optical fibers. Reproduced with permission from [15], copyright Informa PLC, 2017.

As can be seen, among glass fibers, chalcogenide glass is the only one with a transparent domain paving the Mid-IR region. The transmission varies with the constituting chalcogen elements, such as sulfur, selenium, and tellurium [16], as shown in Figure 2. Thus, As–S fiber can transmit from 1 to 6.5 µm [17], As–Se fiber from 1.5 to 10 µm [18], and Te-based fibers, due to heavy atomic weight, can transmit further than 14 µm. In terms of optical nonlinearity, chalcogenide glasses possess a nonlinear refractive index that is 2 to 3 orders of magnitude higher than that of silica [16]. These nonlinear optical properties are even enhanced in small-core single-mode fibers.

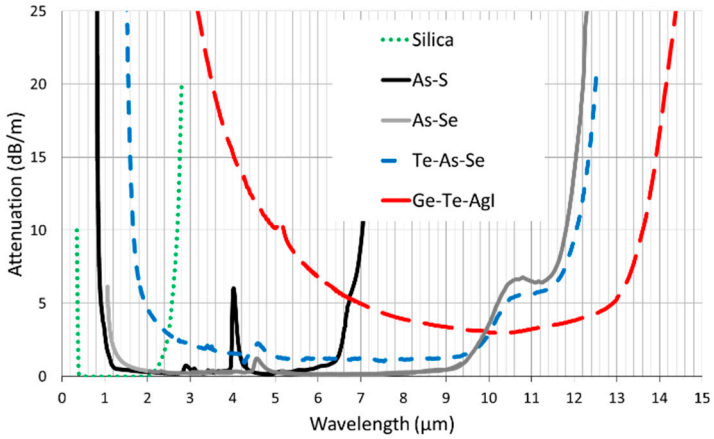

Figure 2. Mid-infrared attenuation of chalcogenide optical fibers in comparison to silica attenuation.

In microstructured optical fibers (MOF), the mode of the light propagating in the fiber is determined by the diameter of the air holes (d) and the distance between air holes (Λ), as depicted in Figure 3. Thus, single-mode guiding regardless of the wavelength can be achieved in MOF, as long as the d/Λ ratio is less than 0.42 [19,20]. Also, by reducing the diameter of the core in MOF, the nonlinearity can be increased and the zero-dispersion wavelength (ZDW) can be controlled over a wide range of wavelengths [21]. Indeed, in order to obtain an efficient supercontinuum source, the fiber has to be pumped close to the ZDW. One of the main advantages of MOFs is to obtain strong flexibility in dispersion modification. The intrinsic ZDWs of chalcogenide glasses are normally located beyond 5 μm, where it is difficult to find available powerful laser pump sources, not to mention fiber lasers. Then, it would be beneficial to shift the ZDW to a shorter wavelength: 1.55 μm for the telecom wavelength, 2 μm, or at least less than 4 μm.

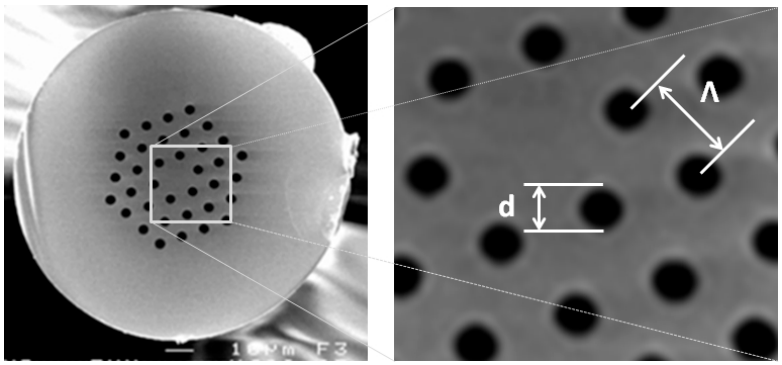

Figure 3. Cross section of a chalcogenide microstructured optical fiber. d: hole size, Λ: distance between the hole (also called "pitch").

For example, by altering the core diameter and with the microstructured geometry, a suspended-core chalcogenide As_2S_3 fiber with a ZDW blue-shifted to around 2 μm was realized [11], whereas the ZDW of the bulk glass is around 5 μm. In this study, the simulated results were confirmed by experimental measurements. Besides, in a Ge–As–Se system [22], where the ZDW of the bulk material is around 7 μm, a microstructured fiber with a ZDW blue-shifted to 3.6 μm was achieved by tapering the fiber core diameter from 12 to 6 μm [22].

Therefore, chalcogenide MOFs combine a broad Mid-IR transmission, high nonlinearity, single-mode guiding, and dispersion tunability, which open up the way to the generation of Mid-IR supercontinua.

3. Fabrications of Chalcogenide Fibers

In order to achieve a broad-bandwidth Mid-IR supercontinuum generation, chalcogenide glass has to be synthesized under vacuumed conditions and purified to avoid optical absorption caused by the presence of chemical bonds such as O–H, Se–H, and As–O, or impurities such as CO_2 and H_2O. To date, several purification methods have been reported, such as the purification of raw material before synthesis [23] or using microwave treatment before synthesis [24]. Also, distillation of the glass after synthesis in the presence of chemical getters proved to be efficient in reducing optical losses in fibers [25]. This last process consists of the addition of halides (such as $TeCl_4$) and metals (such as Mg or Al) to the charge before synthesis. During the melting of the charge, metals will react with oxygen-based pollutants, while halides will react with hydrogen and carbon impurities. The byproducts of this reaction are either refractory or volatile, allowing for their removal by distillation of the glass.

Standard chalcogenide fibers exhibit a step-index profile that can be achieved by implementing two different fabrication methods: the "rod-in-tube" method and the double-crucible method [26–28]. The first technique allows a better control of the fiber-core size, and consequently of the core-clad

ratio [21,29,30]. The second one permits a better control of the core–clad interface [31,32], and commercial step-index chalcogenide fibers have been fabricated by using this technique. Microstructured optical fibers have been obtained with a variety of different glasses, including chalcogenide glasses [33,34]. In 2000, the first chalcogenide MOF, with a Ga–La–S composition, was successfully fabricated by using the "stack-and-draw" technique originally utilized for making silica MOF, yet guidance of light was not observed [33]. Later on, light propagation in chalcogenide MOFs based on sulfur and selenide was realized [35,36]. Then, in 2006, single-mode propagation in a chalcogenide MOF with Ge–Ga–Sb–S composition was reported [34]. Propagation losses of the fiber were quite high, between 15 and 20 dB m^{-1} at 1.55 µm; this was attributed to the poor quality of chalcogenide glass preforms prepared by the "stack-and-draw" method [37]. Indeed, it has been shown that important defects at the interfaces between the chalcogenide capillaries constituting the stack induce strong optical losses [37].

Consequently, other fabrication methods had to be developed for chalcogenide glasses. For example, the geometry of chalcogenide MOF can be realized by the "drilling method" or "casting method". The "drilling method" exploits mechanical drilling in chalcogenide glass preforms to create various geometrical structures. In order to avoid structure destruction, the position of the holes and the friction between glass and drills have to be precisely controlled. Besides, for the protection of the inner side of the holes, it is necessary to optimize the rotation speed and the force applied by the drills [38]. For the "casting method", a mold made of silica capillaries threaded in hexagonal silica guides is designed with the desired distribution of holes. Then, the chalcogenide glass, which has been heated to a quasi-liquid state, is poured into the mold. Afterward, the mold–glass ensemble is quenched in air and annealed. The silica tube and capillaries, which are still inside the MOF preform at this stage, are removed with a diamond tool and soaking in 40% concentrated hydrofluoric acid [39]. Both methods have been tested for making monolithic preforms suitable for obtaining microstructured optical fibers [38–40].

4. Supercontinuum Generation in Chalcogenide MOFs

As one of the promising applications of chalcogenide fibers, Mid-IR supercontinuum generation has been investigated extensively with both step-index and microstructured chalcogenide fibers [41–44].

The first generation of supercontinuum was demonstrated in 2006 for chalcogenide MOFs [36]. One meter of a selenide-based chalcogenide MOF was pumped by a Ti:sapphire laser, with an output wavelength at 2.5 µm and pulse duration and pulse energy of 100 fs and 100 pJ, respectively. The experimental results displayed in Figure 4 show that effective wavelength broadening can be achieved through pumping around the ZDW or the anomalous region [1] of the fiber.

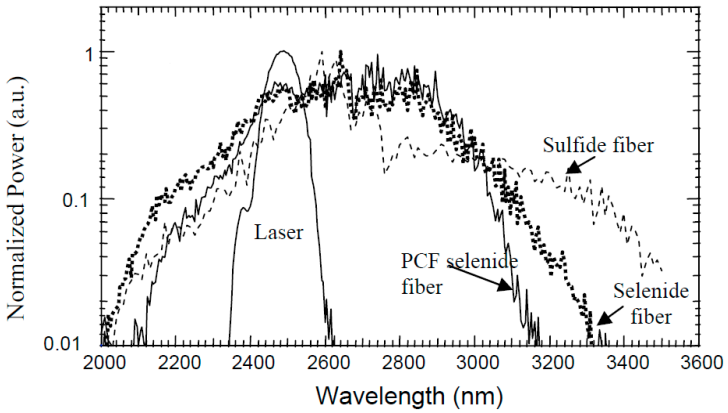

Figure 4. Output spectrum of supercontinuum generated in chalcogenide microstructured optical fibers made by the stack and draw technique. Reproduced with permission from [36], copyright INOE, 2006.

Later in 2010, M. El-Amraoui et al. reported the fabrication of the first As_2S_3 chalcogenide MOFs with a suspended core. Instead of the "stack-and-draw" method, mechanical drilling was used to prepare the fiber preform. By pumping a 45-m-long section of MOF with an 8-ps mode-locked laser at around 1.55 µm, a continuum covering more than 200 nm from 1450 to over 1700 nm was obtained [11].

Several other pumping schemes have been investigated to generate Mid-IR supercontinua. In 2016, Petersen et al. used a two-cascading configuration, based on a 1.55-µm laser-diode-pumped thulium-doped silica fiber and a Zr–Ba–La–Al–Na fluoride (ZBLAN) fiber, to pump a chalcogenide MOF, which generated a Mid-IR supercontinuum up to 4.4 µm [45]. By comparing the output spectra of ZBLAN fibers with different chromatic dispersions, it was concluded that solitons located in the long-wavelength part of the pump are essential for the effective generation of the supercontinuum. This was corroborated by a series of simulations. The spectrum of the supercontinuum was extended to 7 µm with a total output power of 6.5 mW. Then, in 2017, Petersen et al. demonstrated a Mid-IR SC generation from a tapered large-mode-area chalcogenide MOF [22]. The tunable Mid-IR pump light utilized in the experiment was achieved by combining a tunable seed laser and a 1.04-µm mode-locked Yb:KYW (ytterbium-doped potassium yttrium tungstate crystal) solid-state laser into periodically-poled MgO:$LiNbO_3$ crystals to obtain quasi-phase-matched parametric anti-Stokes generation from 3.7 to 4.5 µm. In order to increase the spectral broadening and reduce the confinement losses, tapered fibers with a diameter of 15.1 µm and shorter lengths before and after the taper, with length before taper (L_{bt}) of 7.5 cm and length after taper (L_{at}) of 4.5 cm, was utilized in the experiment. At the end, an output spectrum from 1 to 11.5 µm with an average output power of 35.4 mW was obtained, as shown in Figure 5.

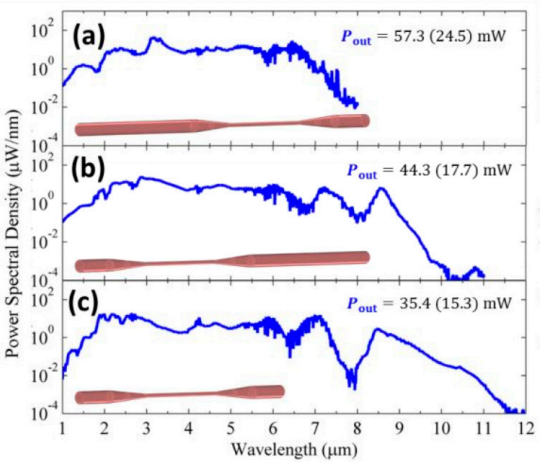

Figure 5. Supercontinuum spectra obtained from a tapered chalcogenide MOF, for three different configurations of lengths of nontapered zones at the input and output of the fiber (in brown color). (**a**) Lbt = 25 cm, Lat = 7.5 cm; (**b**) Lbt = 7.5 cm, Lat = 25 cm; (**c**) Lbt = 7.5 cm, Lat = 4 cm. (With L_{bt}: length before taper, L_{at}: length after taper and P_{out}: average integrated out power). Adapted with permission from ref [22], copyright The Optical Society, 2017.

Besides, hybrid chalcogenide MOFs were fabricated by Cheng et al. to generate a Mid-IR supercontinuum [46]. The hybrid MOF has been made with four $AsSe_2$ capillaries and inserted into an As_2S_5 glass tube (Figure 6a). The high refractive index difference (around 0.61) between the core and the cladding would improve light confinement in the fiber, which was the original intent of the fiber designing. As for the pump light, a tunable optical parametric oscillator (OPO) emitting 200-fs pulses at a repetition of 80 MHz was employed. For the purpose of extending the output spectra, different pump wavelengths: 3062 nm, 3241 nm, and 3389 nm, located at positions far from the ZDW in the normal dispersion range, close to the ZDW in the normal dispersion range, and close to ZDW in the anomalous dispersion range, respectively, were used to pump the 2-cm-long hybrid MOF. Compared

to the other wavelengths used, the broader spectrum from 1250 to 5370 nm was obtained by pumping at 3.389 µm (Figure 6b).

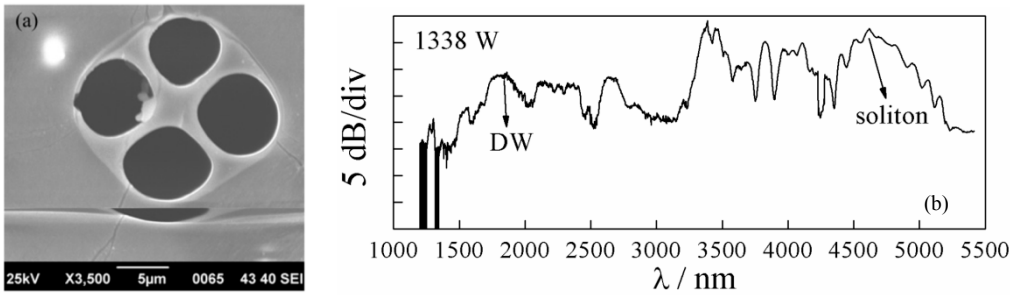

Figure 6. (**a**) Cross section of the $AsSe_2$–As_2S_5 hybrid MOF. (**b**) Output spectrum of the mid-infrared (Mid-IR) supercontinuum obtained by pumping at 3389 nm. Adapted with permission from ref [46], copyright The Optical Society, 2014.

A summary of supercontinua generated in chalcogenide MOF with different glass compositions, geometries, and pumping regimes discussed in this article are presented in Table 1. The broader supercontinuum spectrum obtained in a chalcogenide MOF presents a spectral coverage from 1 to 11.5 µm with an average output power of 35 mW. The higher output power obtained in a chalcogenide MOF reaches more than 57 mW in the 1–8 µm wavelength range.

Table 1. Mid-IR supercontinuum generation obtained in chalcogenide MOFs.

Fiber Composition	Spectral Coverage	Pump Wavelength (Pulse Duration)	Output Average Power	References
As_2S_3	2.1–3.2 µm	2.5 µm (100 fs)	-	[36]
As_2S_3	1–2.6 µm	1.55 µm (400 fs)	-	[38]
$AsSe_2$-As_2S_5	1.2–5.37 µm	3.3 µm (200 fs)	214 mW (input)	[46]
$As_{38}Se_{62}$	1.9–7.1 µm	Cascading from 1.55 to 4.5 µm (3 ns)	6.5 mW	[45]
$Ge_{10}As_{22}Se_{68}$	1–11.5 µm	4 µm (252 fs)	35.4 mW	[22]
$Ge_{10}As_{22}Se_{68}$	1–8 µm	4 µm (252 fs)	57.3 mW	[22]

The supercontinuum obtained by cascading SC in different materials [45] is probably the most promising way for the future. Indeed, this all-fiber approach can lead to more stable, versatile, robust, and compact Mid-IR sources with easy handling. Also, it is well known that more stable and better coupling efficiencies can be obtained with fibers in comparison to free space coupling.

5. Applications of Mid-IR Supercontinuum Generation

Thanks to a broad Mid-IR range coverage, high coherence, and good beam quality, Mid-IR supercontinuum sources are potential candidates for a variety of applications in domains such as spectroscopy, sensing, biology, metrology, and spectral imaging [43,47].

As an example of this, the IR signature of propanol and acetone has been detected by fibers evanescent wave spectroscopy (FEWS) using a chalcogenide MOF [47]. In this experiment, it was demonstrated that an exposed-core chalcogenide MOF, as shown in Figure 7, can be more sensitive to the environment than classical single-index fibers, such as those used in ref. [23].

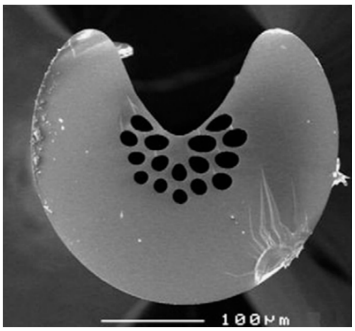

Figure 7. Scanning electron microscope image of an exposed-core chalcogenide microstructured optical fiber (MOF). Reproduced with permission from [47], copyright Elsevier, 2013.

Mid-IR spectral imaging, combined with data mining algorithms, has been utilized as an aid for diagnosing some types of cancers [48–51]. The acquisition speed and penetration depth of traditional Mid-IR spectral imaging is subject to low brightness and lack of flexibility for the delivery and detection of light [52]. Therefore, intense laser sources with high signal-to-noise ratios become an ideal choice for rapid acquisition through the Mid-IR range. Quantum cascade lasers (QCL) were once used in Mid-IR spectral imaging systems to reduce the acquisition time, but the limited frequency coverage of QCLs cannot satisfy the diagnostic requirements and maintain, at the same time, the simplicity of the system at a reasonable cost. Thus, supercontinuum sources were selected for broadband Mid-IR spectral imaging. For example, ZBLAN-fluoride-fiber-based supercontinuum sources, with a 2–4.5 µm spectral range, were selected to be integrated into Mid-IR spectral imaging systems demonstrated in the past few years [53–55].

In 2012, Dupont et al. presented, for the first time, a high-resolution contact-free infrared microscope. By using a 1900-nm fiber laser to pump 10 m of ZBLAN fiber, the generated supercontinuum spanned from 1.4 to 4.0 µm. The system was tested by a mixture of oil and water and resolutions of 35 µm and 25 µm for the water absorption image and oil absorption image were obtained, respectively, as shown in Figure 8 [53].

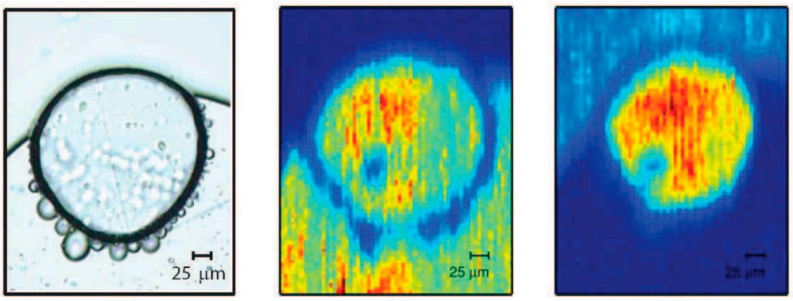

Figure 8. (**a**) Optical microscope image of oil–water mixture; (**b**,**c**) IR microscope image obtained at wavelengths corresponding to high absorption of water and oil, respectively. Adapted with permission from ref [53], copyright The Optical Society, 2012.

In 2017, Farries et al. reported a mid-infrared spectral imaging system for the rapid assessment of cells for cytological diagnosis, consisting of a ZBLAN-fiber-based supercontinuum source, a fast acousto-optic tunable filter (AOTF), and a high-resolution thermal camera. The AOTF enables the system to record a 100-wavelengths image cube and 300 k pixels in 2 s, so that it can be used to test the cells of a living person. By comparison, the system proved to have a higher spectral resolution than a Fourier transform infrared (FTIR) system. Restricted by the filter inside the thermal camera and the range of the supercontinuum source, collection of samples of colon cells could be imaged, nevertheless, in the 2.87–3.7 µm spectral range [54].

Hence, in the later studies, chalcogenide MOFs were chosen to replace ZBLAN fibers. In 2018, Peterson et al. designed the first Mid-IR spectral imaging system in the long-wavelength region using SC generation [52]. The system consisted of a point scanning device and a chalcogenide fiber-based supercontinuum. The supercontinuum source could deliver light from 2 to 7.5 µm with an output power of 25 mW, which enabled the system to collect sample information from 5.7 to 7.3 µm, in the diagnostic fingerprint region [52]. Figure 9 presents the first mid-IR spectral image obtained with an SC containing wavelengths longer than 4 µm. The Mid-IR image obtained at 6.03 µm (Figure 9c) is compared to classical histologic analysis (visible images, Figure 9a,b) [52].

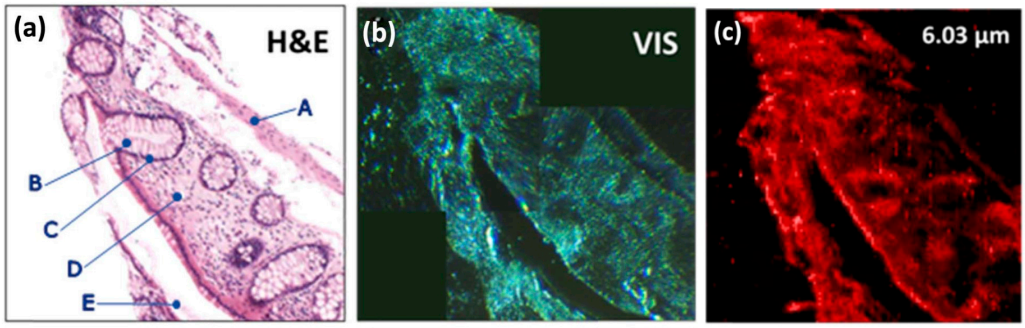

Figure 9. (**a**) Confocal image from histological analysis using gold standard hematoxylin and eosin (H&E); (**b**) visible light transmission image of the sample; (**c**) Mid-IR absorbance image. Adapted with permission from ref [52], copyright The Optical Society, 2018.

6. Conclusions

The main interest in chalcogenide MOFs is to combine the broad Mid-IR transmission range of chalcogenide glasses with the highly tunable optical properties of microstructured fibers. Via the comparison of different classes of glasses and fiber structures, we can establish that chalcogenide MOFs are surely an optimal medium for efficient supercontinuum generation in the Mid-IR region.

Since the first generations of supercontinua in chalcogenide fibers, the power and the bandwidth obtained have increased dramatically, now reaching 400 mW in step-index fibers and 55 mW in chalcogenide MOFs, with mid-IR wavelengths generated up to 12 µm. Consequently, we can say that the concept of generating supercontinua in chalcogenide fibers has been proved. It has been shown also that the power obtained is now sufficient for applications such as spectroscopy or imaging.

However, some strong challenges remain to be tackled before compact and robust all-fiber sources are achieved. Setting innovative and efficient pump schemes, achieving fiber splicing, and improving the damage threshold are examples of those challenges. When overcome, it will be possible to take full advantage of the unique and versatile optical properties of chalcogenide microstructured fibers in the infrared spectrum, such as endless single-mode propagation, high numerical aperture, and readily tunable dispersion.

Author Contributions: Y.W., J.T., and J.-L.A. have written the paper together and M.M. has contributed for constituting the bibliography.

Funding: The article has been supported by the SUPUVIR ITN project. This project has received funding from the European Union's Horizon 2020 research and innovation program under grant agreement No. 722380.

Conflicts of Interest: The authors declare no conflict of interest.

References

1. Dudley, J.M.; Genty, G.; Coen, S. Supercontinuum generation in photonics crystal fiber. *Rev. Mod. Phys.* **2006**, *78*, 1135–1184. [CrossRef]
2. Schliesser, A.; Picqué, N.; Hänsch, T.W. Mid-infrared frequency combs. *Nat. Photonics* **2012**, *6*, 440–449. [CrossRef]

3. Swiderski, J.; Michalska, M. Mid-infrared supercontinuum generation in a single-mode thulium-doped fiber amplifier. *Laser Phys. Lett.* **2013**, *10*, 035105. [CrossRef]
4. Yin, K.; Zhu, R.; Zhang, B.; Jiang, T.; Chen, S.; Hou, J. Ultrahigh-brightness, spectrally-flat, short-wave infrared supercontinuum source for long-range atmospheric applications. *Opt. Express* **2016**, *24*, 20010–20020. [CrossRef] [PubMed]
5. Lægsgaard, J.; Tu, H. How long wavelengths can one extract from silica-core fibers? *Opt. Lett.* **2013**, *38*, 4518–4521. [CrossRef] [PubMed]
6. Savelii, I.; Mouawad, O.; Fatome, J.; Kibler, B.; Désévédavy, F.; Gadret, G.; Jules, J.-C.; Bony, P.-Y.; Kawashima, H.; Gao, W.; et al. Mid-infrared 2000-nm bandwidth supercontinuum generation in suspended–core microstructuered Sulfide and Tellurite optical fibers. *Opt. Express* **2012**, *20*, 27083–27093. [CrossRef] [PubMed]
7. Domachuk, P.; Wolchover, N.A.; Cronin-Golomb, M.; Wang, A.; George, A.K.; Cordeiro, C.M.B.; Knight, J.C.; Omenetto, F.G. Over 4000 nm Bandwidth of Mid-IR Supercontinuum Generation in sub-centimeter Segments of Highly Nonlinear Tellurite PCFs. *Opt. Express* **2008**, *16*, 7161–7168. [CrossRef] [PubMed]
8. Théberge, F.; Daigle, J.-F.; Vincent, D.; Mathieu, P.; Fortin, J.; Schmidt, B.E.; Thiré, N.; Légaré, F. Mid-infrared supercontinuum generation in fluoroindate fiber. *Opt. Lett.* **2013**, *38*, 4683–4685. [CrossRef] [PubMed]
9. Qin, G.; Yan, X.; Kito, C.; Liao, M.; Chaudhari, C.; Suzuki, T.; Ohishi, Y. Ultrabroadband supercontinuum generation from ultraviolet to 6.28 μm in a fluoride fiber. *Appl. Phys. Lett.* **2009**, *95*, 161103. [CrossRef]
10. Petersen, C.R.; Møller, U.; Kubat, I.; Zhou, B.; Dupont, S.; Ramsay, J.; Benson, T.; Sujecki, S.; Abdel-Moneim, N.; Tang, Z.; et al. Mid-infrared supercontinuum covering the 1.4–13.3 μm molecular fingerprint region using ultra-high NA chalcogenide step-index fibre. *Nat. Photonics* **2014**, *8*, 830–834. [CrossRef]
11. El-Amraoui, M.; Fatome, J.; Jules, J.C.; Kibler, B.; Gadret, G.; Fortier, C.; Smektala, F.; Skripatchev, I.; Polacchini, C.F.; Messaddeq, Y.; et al. Strong infrared spectral broadening in low-loss As-S chalcogenide suspended core microstructured optical fibers. *Opt. Express* **2010**, *18*, 4547–4556. [CrossRef] [PubMed]
12. Cheng, T.; Kanou, Y.; Deng, D.; Xue, X.; Matsumoto, M.; Misumi, T.; Suzuki, T.; Ohishi, Y. Fabrication and characterization of a hybrid four-hole $AsSe_2$-As_2S_5 microstructured optical fiber with a large refractive index difference. *Opt. Express* **2014**, *22*, 13322–13329. [CrossRef] [PubMed]
13. Martinez, R.A.; Plant, G.; Guo, K.; Janiszewski, B.; Freeman, M.J.; Maynard, R.L.; Islam, M.N.; Terry, F.L.; Alvarez, O.; Chenard, F.; et al. Mid-infrared supercontinuum generation from 1.6 to >11 um using concatenated step-index fluoride and chalcogenide fibers. *Opt. Lett.* **2018**, *43*, 296–299. [CrossRef] [PubMed]
14. Yang, W.; Zhang, B.; Xue, G.; Yin, K.; Hou, J. Thirteen watt all-fiber mid-infrared supercontinuum generation in a single mode ZBLAN fiber pumped by a 2 μm MOPA system. *Opt. Lett.* **2014**, *39*, 1849–1852. [CrossRef] [PubMed]
15. Troles, J.; Brilland, L.; Caillaud, C.; Adam, J.L. Original designs of chalcogenide microstuctured optical fibers. *Adv. Device Mater.* **2017**, *3*, 7–13. [CrossRef]
16. Savage, J.A. Optical properties of chalcogenide glasses. *J. Non-Cryst. Solids* **1982**, *47*, 101–116. [CrossRef]
17. Snopatin, G.; Shiryaev, V.; Plotnichenko, V.; Dianov, E.; Churbanov, M. High-purity chalcogenide glasses for fiber optics. *Inorg. Mater.* **2009**, *45*, 1439–1460. [CrossRef]
18. Churbanov, M.F. High-purity chalcogenide glasses as materials for fiber optics. *J. Non-Cryst. Solids* **1995**, *184*, 25–29. [CrossRef]
19. Birks, T.A.; Knight, J.C.; Russell, P.S. Endlessly single-mode photonic crystal fiber. *Opt. Lett.* **1997**, *22*, 961–963. [CrossRef] [PubMed]
20. Renversez, G.; Bordas, F.; Kuhlmey, B.T. Second mode transition in microstructured optical fibers: Determination of the critical geometrical parameter and study of the matrix refractive index and effects of cladding size. *Opt. Lett.* **2005**, *30*, 1264–1266. [CrossRef] [PubMed]
21. Ballato, J.; Ebendorff-Heidepriem, H.; Zhao, J.; Petit, L.; Troles, J. Glass and Process Development for the Next Generation of Optical Fibers: A Review. *Fibers* **2017**, *5*, 11. [CrossRef]
22. Petersen, C.; Engelsholm, R.D.; Markos, C.; Brilland, L.; Caillaud, C.; Trolès, J.; Bang, O. Increased mid-infrared supercontinuum bandwidth and average power by tapering large-mode-area chalcogenide photonic crystal fibers. *Opt. Express* **2017**, *25*, 15336–15347. [CrossRef] [PubMed]
23. Hocdé, S.; Boussard-Plédel, C.; Fonteneau, G.; Lucas, J. Chalcogens based glasses for IR fiber chemical sensors. *Solid State Sci.* **2001**, *3*, 279–284. [CrossRef]

24. Danto, S.; Thompson, D.; Wachtel, P.; Musgraves, J.D.; Richardson, K.; Giroire, B. A comparative study of purification routes for As_2Se_3 chalcogenide glass. *Int. J. Appl. Glass Sci.* **2013**, *4*, 31–41. [CrossRef]
25. Shiryaev, V.S.; Churbanov, M.F. Recent advances in preparation of high-purity chalcogenide glasses for mid-IR photonics. *J. Non-Cryst. Solids* **2017**, *475*, 1–9. [CrossRef]
26. Churbanov, M.F.; Shiryaev, V.S.; Scripachev, I.V.; Snopatin, G.E.; Gerasimenko, V.V.; Smetanin, S.V.; Fadin, I.E.; Plotnichenko, V.G. Optical fibers based on As-S-Se glass system. *J. Non-Cryst. Solids* **2001**, *284*, 146–152. [CrossRef]
27. Kim, W.H.; Nguyen, V.Q.; Shaw, L.B.; Busse, L.E.; Florea, C.; Gibson, D.J.; Gattass, R.R.; Bayya, S.S.; Kung, F.H.; Chin, G.D.; et al. Recent progress in chalcogenide fiber technology at NRL. *J. Non-Cryst. Solids* **2016**, *431*, 8–15. [CrossRef]
28. Kobelke, J.; Kirchhof, J.; Scheffler, M.; Schwuchow, A. Chalcogenide glass single mode fibres—Preparation and properties. *J. Non-Cryst. Solids* **1999**, *256*, 226–231. [CrossRef]
29. Houizot, P.; Smektala, F.; Couderc, V.; Troles, J.; Grossard, L. Selenide glass single mode optical fiber for nonlinear optics. *Opt. Mater.* **2007**, *29*, 651–656.
30. Troles, J.; Niu, Y.; Duverger-Arfuso, C.; Smektala, F.; Brilland, L.; Nazabal, V.; Moizan, V.; Desevedavy, F.; Houizot, P. Synthesis and characterization of chalcogenide glasses from the system Ga-Ge-Sb-S and preparation of a single-mode fiber at 1.55 µm. *Mater. Res. Bull.* **2008**, *43*, 976–982. [CrossRef]
31. Chenard, F.; Alvarez, O.; Moawad, H. MIR chalcogenide fiber and devices. In Proceedings of the SPIE Conference on Optical Fibers and Sensors for Medical Diagnostics and Treatment Applications XV, San Francisco, CA, USA, 7–12 February 2015; Volume 9317, p. 93170B.
32. Lafond, C.; Couillard, J.-F.; Delarosbil, J.-L.; Sylvain, F.; de Sandro, P. Recent improvements on mid-IR chalcogenide optical fibers. In Proceedings of the SPIE 40th Conference on Infrared Technology and Applications XL, Batimore, MD, USA, 5–9 May 2014; Volume 9070, p. 90701C.
33. Monro, T.M.; West, Y.D.; Hewak, D.W.; Broderick, N.G.R.; Richardson, D.J. Chalcogenide holey fibres. *Electron. Lett.* **2000**, *36*, 1998–2000. [CrossRef]
34. Brilland, L.; Smektala, F.; Renversez, G.; Chartier, T.; Troles, J.; Nguyen, T.N.; Traynor, N.; Monteville, A. Fabrication of complex structures of Holey fibers in chalcogenide glass. *Opt. Express* **2006**, *14*, 1280–1285. [CrossRef] [PubMed]
35. Le Person, J.; Smektala, F.; Chartier, T.; Brilland, L.; Jouan, T.; Troles, J.; Bosc, D. Light guidance in new chalcogenide holey fibres from GeGaSbS glass. *Mater. Res. Bull.* **2006**, *41*, 1303–1309. [CrossRef]
36. Sanghera, J.S.; Aggarwal, I.D.; Shaw, L.B.; Florea, C.M.; Pureza, P.; Nguyen, V.Q.; Kung, F. Nonlinear properties of chalcogenide glass fibers. *J. Optoelectron. Adv. Mater.* **2006**, *8*, 2148–2155.
37. Brilland, L.; Troles, J.; Houizot, P.; Desevedavy, F.; Coulombier, Q.; Renversez, G.; Chartier, T.; Nguyen, T.N.; Adam, J.L.; Traynor, N. Interfaces impact on the transmission of chalcogenide photonic crystal fibres. *J. Ceram. Soc. Jpn.* **2008**, *116*, 1024–1027. [CrossRef]
38. El-Amraoui, M.; Gadret, G.; Jules, J.C.; Fatome, J.; Fortier, C.; Désévédavy, F.; Skripatchev, I.; Messaddeq, Y.; Troles, J.; Brilland, L.; et al. Microstructured chalcogenide optical fibers from As_2S_3 glass: Towards new IR broadband sources. *Opt. Express* **2010**, *18*, 26655–26665. [CrossRef] [PubMed]
39. Coulombier, Q.; Brilland, L.; Houizot, P.; Chartier, T.; Nguyen, T.N.; Smektala, F.; Renversez, G.; Monteville, A.; Méchin, D.; Pain, T.; et al. Casting method for producing low-loss chalcogenide microstructured optical fibers. *Opt. Express* **2010**, *18*, 9107–9112. [CrossRef] [PubMed]
40. Zhang, P.; Zhang, J.; Yang, P.; Dai, S.; Wang, X.; Zhang, W. Fabrication of chalcogenide glass photonic crystal fibers with mechanical drilling. *Opt. Fiber Technol.* **2015**, *26*, 176–179. [CrossRef]
41. Hudson, D.D.; Antipov, S.; Li, L.; Alamgir, I.; Hu, T.; El Amraoui, M.; Messaddeq, Y.; Rochette, M.; Jackson, S.D.; Fuerbach, A. Toward all-fiber supercontinuum spanning the mid-infrared. *Optica* **2017**, *4*, 1163–1166. [CrossRef]
42. Deng, D.H.; Liu, L.; Tuan, H.T.; Kanou, Y.; Matsumoto, M.; Tezuka, H.; Suzuki, T.; Ohishi, Y. Mid-infrared supercontinuum covering 3–10 µm using a As_2Se_3 core and As_2S_5 cladding step-index chalcogenide fiber. *J. Ceram. Soc. Jpn.* **2016**, *124*, 103–105. [CrossRef]
43. Mouawad, O.; Picot-Clemente, J.; Amrani, F.; Strutynski, C.; Fatome, J.; Kibler, B.; Desevedavy, F.; Gadret, G.; Jules, J.C.; Deng, D.; et al. Multioctave midinfrared supercontinuum generation in suspended-core chalcogenide fibers. *Opt. Lett.* **2014**, *39*, 2684–2687. [CrossRef] [PubMed]

44. Gao, W.Q.; El Amraoui, M.; Liao, M.S.; Kawashima, H.; Duan, Z.C.; Deng, D.H.; Cheng, T.L.; Suzuki, T.; Messaddeq, Y.; Ohishi, Y. Mid-infrared supercontinuum generation in a suspended-core As_2S_3 chalcogenide microstructured optical fiber. *Opt. Express* **2013**, *21*, 9573–9583. [CrossRef] [PubMed]
45. Petersen, C.R.; Moselund, P.M.; Petersen, C.; Moller, U.; Bang, O. Spectral-temporal composition matters when cascading supercontinua into the mid-infrared. *Opt. Express* **2016**, *24*, 749–758. [CrossRef] [PubMed]
46. Cheng, T.L.; Kanou, Y.; Xue, X.J.; Deng, D.H.; Matsumoto, M.; Misumi, T.; Suzuki, T.; Ohishi, Y. Mid-infrared supercontinuum generation in a novel $AsSe_2$-As_2S_5 hybrid microstructured optical fiber. *Opt. Express* **2014**, *22*, 23019–23025. [CrossRef] [PubMed]
47. Toupin, P.; Brilland, L.; Boussard-Pledel, C.; Bureau, B.; Mechin, D.; Adam, J.-L.; Troles, J. Comparison between chalcogenide glass single index and microstructured exposed-core fibers for chemical sensing. *J. Non-Cryst. Solids* **2013**, *377*, 217–219. [CrossRef]
48. Baker, R.; Rogers, K.D.; Shepherd, N.; Stone, N. New relationships between breast microcalcifications and cancer. *Br. J. Cancer* **2010**, *103*, 1034–1039. [CrossRef] [PubMed]
49. Kwak, J.T.; Kajdacsy-Balla, A.; Macias, V.; Walsh, M.; Sinha, S.; Bhargava, R. Improving Prediction of Prostate Cancer Recurrence using Chemical Imaging. *Sci. Rep.* **2015**, *5*, 8758. [CrossRef] [PubMed]
50. Fernandez, D.C.; Bhargava, R.; Hewitt, S.M.; Levin, I.W. Infrared spectroscopic imaging for histopathologic recognition. *Nat. Biotechnol.* **2005**, *23*, 469–474. [CrossRef] [PubMed]
51. Nallala, J.; Diebold, M.D.; Gobinet, C.; Bouche, O.; Sockalingum, G.D.; Piot, O.; Manfait, M. Infrared spectral histopathology for cancer diagnosis: A novel approach for automated pattern recognition of colon adenocarcinoma. *Analyst* **2014**, *139*, 4005–4015. [CrossRef] [PubMed]
52. Peterson, C.R.; Prtljaga, N.; Farries, M.; Ward, J.; Napier, B.; Lloyd, G.R.; Nallala, J.; Stone, N.; Bang, O. Mid-infrared multispectral tissue imaging using a chalcogenide fiber supercontinuum source. *Opt. Lett.* **2018**, *43*, 999–1002. [CrossRef] [PubMed]
53. Dupont, S.; Peterson, C.; Thogerson, J.; Agger, C.; Bang, O. IR microscopy utilizing intense supercontinuum light source. *Opt. Express* **2012**, *20*, 4887–4892. [CrossRef] [PubMed]
54. Farries, M.; Ward, J.; Lindsay, I.; Nallala, J.; Moselund, P. Fast hyper-spectral imaging of cytological samples in the mid-infrared wavelength region. In Proceedings of the Conference on Optical Biopsy XV-Toward Real-Time Spectroscopic Imaging and Diagnosis, San Francisco, CA, USA, 28 January–2 February 2017; Volume 10060, p. 100600Y.
55. Borondics, F.; Jossent, M.; Sandt, C.; Lavoute, L.; Gaponov, D.; Hideur, A.; Dumas, P.; Février, S. Supercontinuum-based Fourier transform infrared spectromicroscopy. *Optica* **2018**, *5*, 378–381. [CrossRef]